SMAR 2019 – Fifth Conference on Smart Monitoring,
Assessment and Rehabilitation of Civil Structures

SMAR 2019

EBROG technique to enhance the bond performance of CFRP strips to concrete substrate

Christoph CZADERSKI [1], Niloufar MOSHIRI [1, 2], Ardalan HOSSEINI [1],
Davood MOSTOFINEJAD [2], Masoud MOTAVALLI [1]
[1] Empa, Structural Engineering, Dübendorf, Switzerland
[2] Isfahan University of Technology (IUT), Isfahan, Iran

Contact e-mail: christoph.czaderski@empa.ch

ABSTRACT: A well accepted retrofit technique in the civil industry is the application of carbon fiber reinforced polymer (CFRP) reinforcement by using structural epoxy adhesives to strengthen existing reinforced concrete members. Usually, the concrete surface has to be ground or sand blasted, prior to the application of CFRP strips. Although the technique is quite fast and easy, its major problem is the premature debonding failure of the CFRP reinforcement, when the strengthened member is subjected to external loading up to failure. This undesired failure mode occurs because the tensile strength of the concrete is limited.

In this paper, bond performance of a recently introduced technique, called externally bonded reinforcement on grooves (EBROG) is investigated. The technique uses longitudinal grooves cut into the concrete surface in order to better distribute the interfacial shear stresses to deeper layers of concrete substrate, and consequently, to increase the CFRP-to-concrete bond resistance. Sets of lap-shear and four-point beam tests strengthened with the conventional externally bonded reinforcement (EBR) in comparison to EBROG technique are described. Experimental results demonstrated the great potential of EBROG technique for the strengthening of existing concrete structures.

1 INTRODUCTION

The rehabilitation of existing reinforced concrete structures such as buildings and bridges is more and more important because of the large number of existing structures, which are aging or their usage is changing for example due to new owners. A well accepted retrofitting method in the civil industry is the application of carbon fiber reinforced polymer (CFRP) strips by using a two-component adhesive to strengthen existing reinforced concrete structures. CFRP is substantially lighter than steel, has excellent corrosion resistance, tensile and fatigue strength.

1.1 Externally bonded reinforcement (EBR)

Usually, the surface of the concrete has to be ground or sand blasted, and then the CFRP strips are glued to the prepared surface using an adhesive (Figure 1). Although the technique is quite fast and easy, its major problem is the premature debonding failure of the CFRP reinforcement during loading up to failure. This undesired failure mode occurs because the tensile strength of the concrete is limited. Design guidelines for this failure mode are existing and can be found for example in SIA166 (2004) or ACI 440.2R (2017).

1.2 Externally bonded reinforcement on grooves (EBROG)

Mostofinejad et al. (2010) introduced firstly the grooving method (GM). The idea is displayed in Figure 2. Grooves with typical dimensions of 10 × 10 mm are cut in the concrete surface in the longitudinal direction of the CFRP strip. The spacing between the grooves is 15 mm. In order to save working time, the top surface is not ground. The grooves (and the remaining top concrete surface) are filled with the same epoxy adhesive as for the EBR technique.

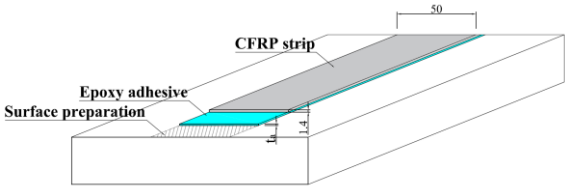

Figure 1. Externally bonded reinforcement (EBR).

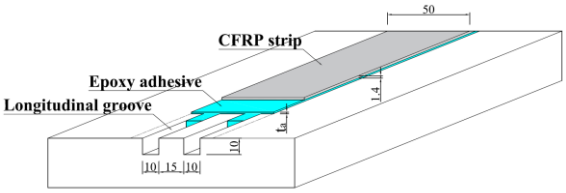

Figure 2. Externally bonded reinforcement on grooves (EBROG).

2 LAP-SHEAR EXPERIMENTS

2.1 Materials

All presented tests were performed with the adhesive S&P Resin 220 and CFRP strips S&P C-Laminate type SM*(150/2000), Austria production, delivered from the Company S&P from Switzerland. The CFRP strip had a width and thickness of 50 mm and 1.4 mm, respectively. The elastic modulus of the CFRP strip was reported by the manufacturer as E_f = 172'500 MPa and from the resin as E_a > 7'100 MPa. The concrete had a maximum aggregate size of 32 mm. Concrete compressive strength for each test is reported in Table 1.

2.2 Test program

As reference, two lap-shear tests were performed using the EBR technique (Figure 1). Furthermore, two lap-shear tests with EBROG technique as shown in Figure 2 were carried out. The overview of the test program with two identical EBR and two identical EBROG lap-shear tests is given in Table 1.

Table 1. Test program of the lap-shear experiments.

Test No.	Concrete cube compressive strength $f_{c,cube}$	Dimension of CFRP strip $b_f \times t_f$	Elastic modulus E_f of CFRP strip
EBR-1	52.3 MPa	50×1.4 mm	172'500 MPa
EBR-2	54.0 MPa	50×1.4 mm	172'500 MPa
EBROG-1	52.3 MPa	50×1.4 mm	172'500 MPa
EBROG-2	54.0 MPa	50×1.4 mm	172'500 MPa

2.3 Test set-up

The lap-shear experiments were performed in a test set-up built at the Structural Engineering Research Laboratory of Empa (see Figure 3). The CFRP strip was glued on a concrete block, which was fixed on the strong floor. The load was applied manually via a hydraulic jack

actuated with a hydraulic hand pump. The jack was fixed on a steel column, which was mounted also on the strong floor. The force was measured with a load-cell, which was attached in line between the hydraulic jack and the clamp for the CFRP strip. Full-field 3D displacements were measured by using a 3D digital image correlation (DIC) measurement system.

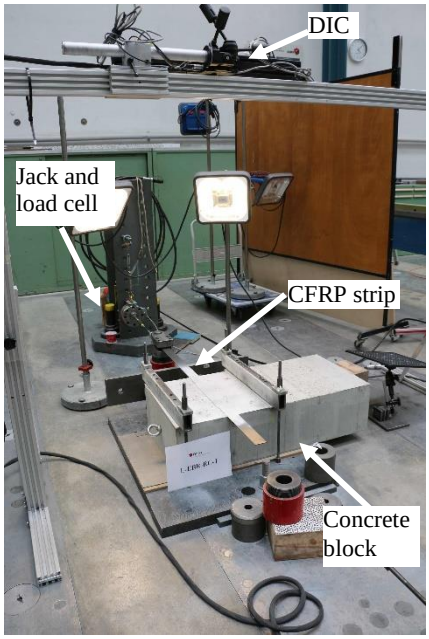

Figure 3. Photo of the test set-up for the lap-shear tests.

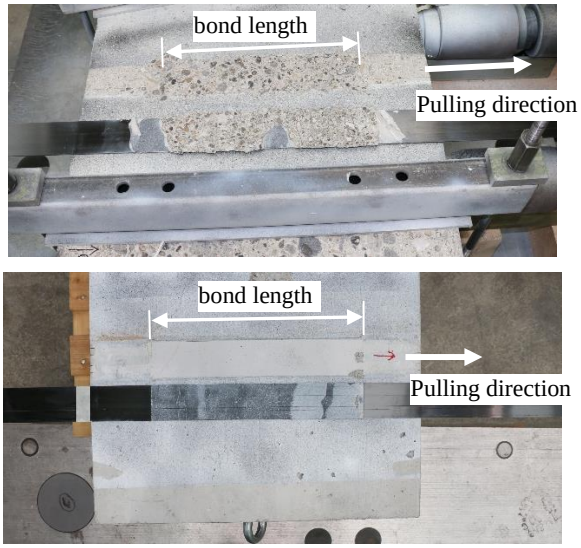

Figure 4. Failure modes: top: EBR-2: debonding failure in the concrete, bottom: EBROG-1: debonding failure in the adhesive layer.

2.4 Experimental results

The two lap-shear tests EBR-1 and EBR-2 failed in the concrete, i.e. debonding, as it is usual in such experiments. A small layer of concrete kept attached on the CFRP strip (Figure 4, top), indicating that the failure was in the concrete substrate. However, the both lap-shear tests EBROG-1 and EBROG-2 failed in the adhesive layer (Figure 4, bottom). A thin layer of epoxy adhesive remained on the CFRP strip after failure, what indicate that the failure was in the adhesive, and no interface debonding between the CFRP strip and the adhesive layer occurred.

The force-slip curves of the four lap-shear tests measured with the DIC system are presented in Figure 5. It is visible that the tests with EBROG showed a significant higher force resistance at the stages of initiation of debonding compared to the EBR tests (the mean value of EBR and EBROG is 28.1 kN and 49.0 kN, which corresponds to a bond strength increase of 74%). However, a large scattering of the test results was observed and more tests are necessary to verify the results.

From the curves presented in Figure 5 in combination with the bilinear bond shear stress-slip model (Figure 6), the behavior during the lap-shear test up to failure can be discussed as following. The first linear part is the elastic behavior. Then, the inclinations of the curves decreases, which indicates that cracks start to develop (the maximum interfacial shear stress is reached). Lastly, the curves are more or less horizontal what means that the initiation of debonding is reached and the debonding process starts. Further loading only increases the

debonded length of the strip. The slips during these load stages are describing deformations of the CFRP strip with zero bond shear stresses (point 2 in Figure 6) and are not important anymore, see Czaderski et al. (2010) for more details. Consequently, specific load stages during the fracture process were selected (see arrows in Figure 5) in order to determine the slip at initiation of debonding. The corresponding forces and slips are given in Table 2.

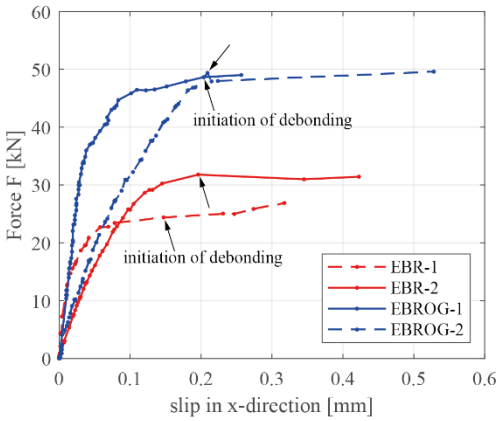

Figure 5. Measured force-slip curves of the four lap-shear tests. Slip at the end of the bond length at x = 300 mm. Arrows indicate the stages of initiation of debonding.

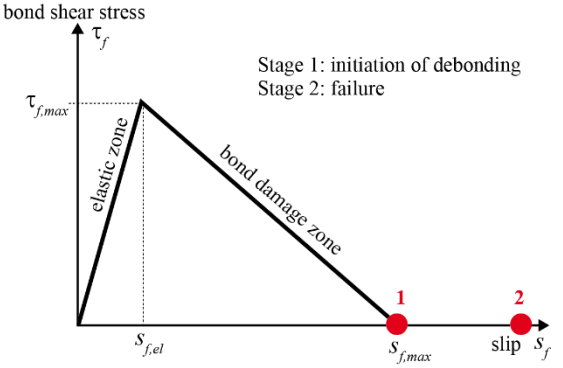

Figure 6. Bilinear bond shear stress-slip relation with designations and explanation of initiation of debonding stage.

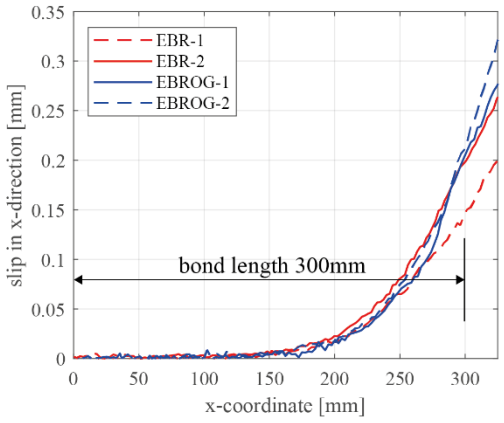

Figure 7. Slip curves along the bond length for the four lap-shear tests at the stages of initiation of debonding indicated in Figure 5 (see arrows).

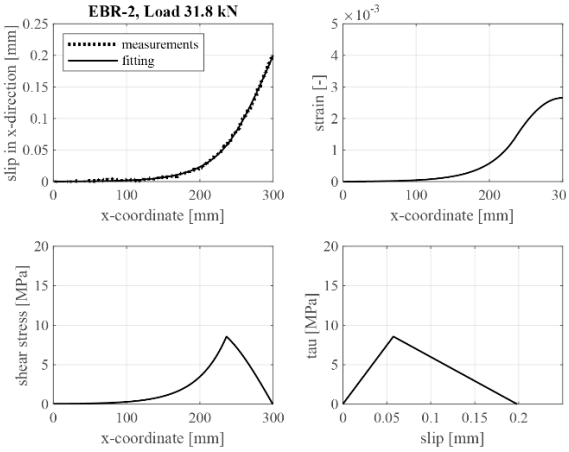

Figure 8. Analytical fitting of the slip curves along the bond length (left above), the corresponding strain (right above), bond shear stress (left bottom) and bond shear stress-slip relation (right bottom) of the test EBR-2 according to the procedure presented in Czaderski et al. (2010).

By using an analytical fitting procedure, the slip, strain and bond shear stress curves were determined from the slip curves measured with the DIC system given in Figure 7. For the sake of brevity, the fitting procedure cannot be described in this paper. The method was presented in Czaderski et al. (2010). The idea is that a bilinear bond shear stress-slip relation (Figure 6) is assumed and the differential equation of bond is solved correspondingly for the two parts of the bond length, i.e., the elastic behavior with a hyperbolic slip shape and the cracked zone with a

trigonometric slip shape. Figure 8 presents the results of the fitting procedure of the test EBR-2 as an example. The determined parameters of all four experiments are listed in Table 2. From the fitting procedure, also the strain and therefore the force can be evaluated. The comparison with the load cell force measurement shows a good agreement of the two measurements, however, the force of EBR-1 and EBROG-2 determined by the slip and fitting procedure is lower as the real force measured with the load cell. The reason for this might be due to the uncertainty of the DIC measurement system and the fitting procedure.

Table 2. Results of the lap-shear experiments and the analyzing procedure (for designations see Figure 6).

Test No.	$F_{load,cell}$ *1	$s_{f,max}$ *2	Parameters determined by fitting of slip curves shown in Figure 6 by using the procedure presented in Czaderski et al. (2010).			
			$s_{f,el}$ *3	$\tau_{f,max}$ *4	$F_{strain,max}$ *5	$F_{strain,max}/F_{load,cell}$
EBR-1	24.4	0.147	0.024	4.8	20.6	0.84
EBR-2	31.8	0.198	0.058	8.6	32.0	1.01
EBROG-1	48.6	0.205	0.123	19.1	48.6	1.00
EBROG-2	49.4	0.213	0.091	13.5	41.7	0.84

*1: Forces measured with load-cell at the initiation of debonding stages indicate in Figure 5.
*2: Slips at loaded end of bond length (x = 300mm) at the initiation of debonding stages.
*3: $s_{f,el}$ = slips at the end of the elastic zone. Determined by fitting of slip curves.
*4: $\tau_{f,max}$ = shear stress at the end of the elastic zone (maximum shear stress). Determined by fitting of slip curves.
*5: $F_{strain,max}$ = force at loaded end of bond length. Determined from strain, which was determined by fitting of slip curves measured with DIC.

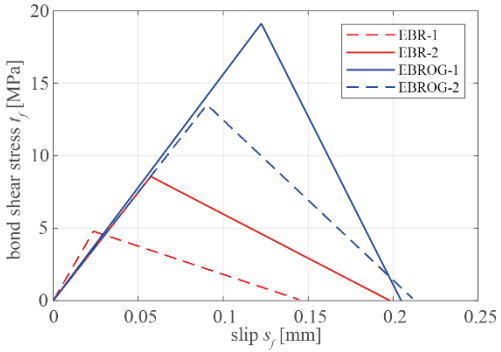

Figure 9. Overview of the bond shear stress-slip relations determined from the four lap-shear tests. Corresponding values are given in Table 2.

All four bond shear stress–slip relations are displayed in Figure 9. Firstly, similar as the force-slip curves in Figure 5, a large scattering of the two EBR and two EBROG tests is visible. The problem discussed above (uncertainty of the DIC measurement system) might be also a reason for the large scattering, specially for the tests EBROG-1 and 2, which actually have almost the same failure load. Anyway, as mentioned before, more tests are necessary to verify the results.

However, a similar elastic stiffness $K_{el}= \tau_{f,max}/s_{f,el}$ in the range of 150-200 N/mm^3 can be observed for the EBR and the EBROG tests. The maximum bond shear stress is significant higher for the EBROG tests compared with the EBR tests (the mean value of EBR and EBROG is 6.7 MPa and 16.3 MPa, respectively), what matches with the force resistances that are also significantly higher for the EBROG tests compared with the EBR test.

3 BEAM EXPERIMENTS

Beside the lap-shear tests, also beam tests were performed. Drawings of the test set-up, the dimensions and the cross-sections of the beams are given in Figure 10. A concrete with a maximum aggregate size of 32 mm was used. Concrete compressive strength for each test is reported in Table 3. The CFRP strips were delivered from the Company S&P from Switzerland and had dimensions and elastic moduli as given in Table 3. The tests were performed with S&P Resin 220. In the same table, the overview of the test program is presented.

The loads were measured with a load cell, the mid-span displacements were measured with two transducers and the strains in the CFRP strip at mid-span were measured with strain gauges.

Table 3. Test program of beam experiments.

Test	Concrete cube compressive strength $f_{c,cube}$	Dimensions of CFRP strip $b_f \times t_f$	Elastic modulus E_f of CFRP strip
Reference Beam	41.6 MPa	-	-
Beam EBR	43.8 MPa	100×1.4 mm	172'500 MPa
Beam EBROG	45.3 MPa	100×1.4 mm	172'500 MPa

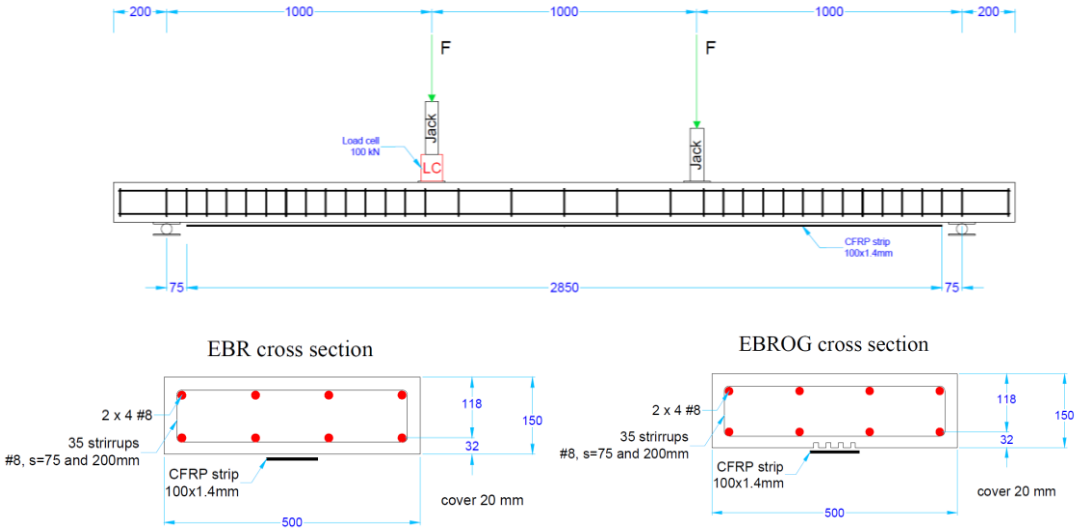

Figure 10. Drawings of beam tests. Beam EBR, Beam EBROG and reference beam without CFRP strip.

3.1 Results

The two beams with CFRP plates failed in debonding of the CFRP strips from the concrete, see Figure 11 for Beam EBR and Figure 12 for Beam EBROG. Beam EBR shows the usual failure mode, which is a crack plane several millimeters parallel to the CFRP strip inside of the concrete surface. However, the debonding failure mode of the Beam EBROG, shown in Figure 12, was clearly different. The failure plane was much deeper inside of the concrete and concrete cover was partly separated. The four grooves filled with epoxy and the internal steel stirrups are partly visible, which indicates that the failure plane was approximately 20 mm deep. Obviously, from such a behavior, a higher bond strength is expected.

Figure 11. Failure mode of Beam EBR: debonding of the CFRP strip from the concrete surface.

Figure 12. Failure mode of Beam EBROG: debonding of the CFRP strip from the concrete surface with partly concrete cover separation.

The measured load–mid-span displacement curves of the three beams are given in Figure 13. Furthermore, maximum force, mid-span displacement, CFRP strip strain and concrete compressive strains are compared in Table 4. The ultimate force increased from 30.7 kN for the Beam EBR to 41.1 kN for the Beam EBROG. The CFRP strip strain of the Beam EBROG was 51% higher at failure compared to the Beam EBR (Figure 14).

Table 4. Results of the beam experiments.

Test	Force F_{max}		Mid-span displacement d_{max}		CFRP strip strain $\varepsilon_{f,max}$		Concrete strain $\varepsilon_{c,max}$	Failure mode
	kN	%	mm	%	‰	%	‰	
Reference Beam	14.9	100	140.5	100	-	-	-3.77	Test was stopped before expected concrete crushing
Beam EBR	30.7	206	49.2	35	5.87	100	-1.58	CFRP strip debonding
Beam EBROG	41.1	276	69.3	49	8.89	151	-2.24	CFRP strip debonding with partly concrete cover separation

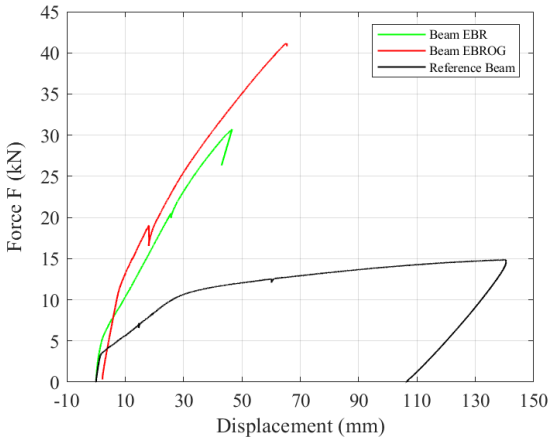

Figure 13. Load–mid-span displacement curves of the three beams.

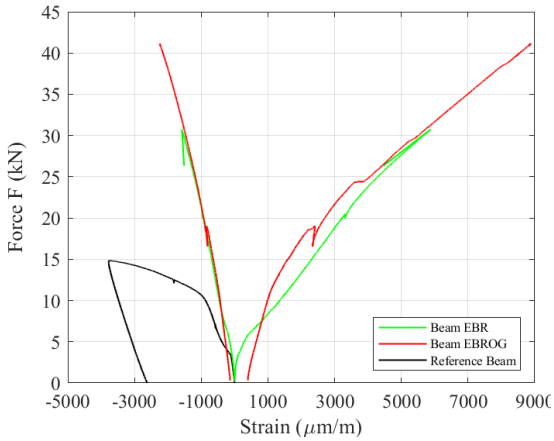

Figure 14. Load–strain in CFRP and concrete at mid-span

4 CONCLUSIONS

In this paper, a preliminary study on a recently introduced new method for the strengthening of concrete structures is presented. The so-called externally bonded reinforcement on grooves (EBROG) technique with longitudinal grooves in the concrete surface increased the bond strength significantly.

The analytical fitting procedure showed an increase of the maximum bond shear stress from a mean value of 6.7 MPa (in EBR joints) to 16.3 MPa by using the EBROG technique, which is 2.4 times higher. The average lap-shear force resistance of the EBROG tests increased 74% compared to that of the EBR tests. The failure load of a CFRP-strengthened beam increased 33% and the utilized strain in the CFRP strip was increased by 51% at debonding failure in the Beam EBROG, compared to the Beam EBR. However, a large scattering of the test results was observed and more tests are necessary to verify the results.

5 ACKNOWLEGMENTS

The financial support and delivery of material of the S&P Clever Reinforcement Company from Seewen in Switzerland is gratefully acknowledged. The second author was financed by the mobility grants received from Iranian Ministry of Science, Research and Technology (MSRT), Iranian National Elites Foundation, and ZHAW (Swiss Leading House for research collaboration with partner institutions) for the visiting research period at Empa.

6 REFERENCES

ACI_440.2R-17, Guide for the design and construction of externally bonded FRP systems for strengthening concrete structures. 2017: *American Concrete Institute*. pp. 116.

Czaderski, C., K. Soudki, and M. Motavalli, Front and Side View Image Correlation Measurements on FRP to Concrete Pull-Off Bond Tests. *Journal of Composites for Construction, ASCE*, 2010. 14(4): p. 451-463.

Mostofinejad, D. and E. Mahmoudabadi, Grooving as alternative method of surface preparation to postpone debonding of FRP laminates in concrete beams. *Journal of Composites for Construction*, 2010. 14(6): p. 804-811.

SIA166, Klebebewehrungen (Externally bonded reinforcement). 2004, Zurich, Switzerland: *Schweizerischer Ingenieur- und Architektenverein, SIA*. pp. 44.